

Investigation of Supercapacitor's Impedance Based on Spectroscopic Measurements

Rodica Negroiu, Paul Svasta, Ciprian Ionescu, Alexandru Vasile

University "Politehnica" of Bucharest, Romania, Center of Technological Electronics and Interconnection Techniques,

UPB-CETTI

rodica.negroiu@cetti.ro

Abstract: Current trends in supercapacitor technology (principally in lowering series discharge resistance) have promoted the devices into roles parallel to, or replacing traditional batteries. In cases where power consumption is low, supercapacitors are an attractive alternative, completely eliminating batteries and further offering higher surge currents. This opens the path towards powering mobile switching circuits, or with high-consumption for short periods.

To power such circuits, the arrangement's limits need to be observed, respectively what can supercapacitors offer in terms of series resistance, self-discharge (parallel) resistance and capacitance.[1]

One of the methods used to determine the after mentioned parameters is Electrochemical Impedance Spectroscopy (EIS).

In the present study we show the determinations on 3 supercapacitors, of 5F, 10 F and 22 F respectively. This is a study seldom published, most EIS determinations being in the range up to 1 F [6] and we feel that EIS determinations for higher capacitances should be known to the community.

Keywords: Supercapacitors, Electrochemical Impedance Spectroscopy- EIS, temperature.

I. Introduction of electrochemical double layer

The double layer of Helmholtz is actually a multiple layer according to the Gouy-Chapman model (Fig. 1.). This multiple layer comprises a Helmholtz internal double layer (PHI) found at the interface between the electrode and the electrolyte solution here are found the adsorbed ions, a Helmholtz external double layer (PHE) in which solvated but that is not absorbed and a diffuse layer that is an area that extends to the mass of the solution.[2]

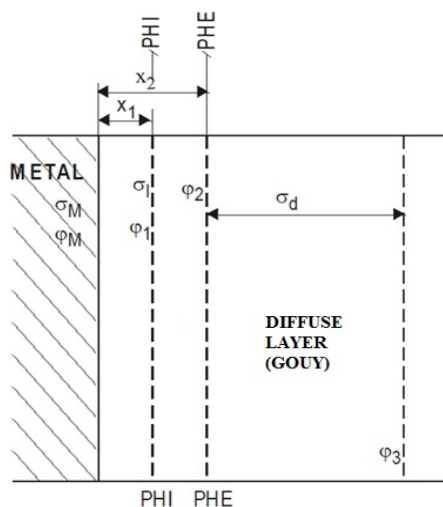


Fig. 1. The model of Gouy-Chapman

An equivalent circuit for modeling supercapacitor based on Gouy-Chapman model can be the circuit Randles such as in the Fig. 2. This circuit includes a combination between faradaic process and the capacitance of double layer.

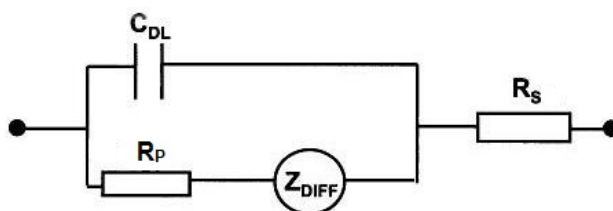


Fig. 2. The equivalent circuit for modeling supercapacitor

The parameters of the circuit presented above are: C_{DL} - the capacitance of double layer, R_p is the charge-transfer resistance, Z_{DIFF} is the Warburg diffusion impedance and R_s that represents the resistance of electrolyte solution:

$$\frac{1}{C_{DL}} = \frac{1}{C_H} + \frac{1}{C_{DIFF}} \quad (1)$$

Where C_H is the capacitance of Helmholtz layer that includes the capacitance of inner plane and capacitance of outer plane, C_{DIFF} is the capacitance of diffuse layer.

$$R_p = \frac{R_G T}{z F i_0} \quad (2)$$

$$Z_{DIFF} = \frac{2 R_G T}{z^2 F^2} \cdot \frac{1-j}{CA\sqrt{2D\omega}} \quad (3)$$

Where i_0 = exchange current density, $F = 96500$ C/mol = Faraday constant, T = absolute temperature in K, $R_G = 8.31$ J/(K mol) = gas constant, z = number of electrons involved, D = diffusion coefficient, C = bulk concentration of the diffusing species (moles/cm³), A = electrode surface area. [3]

II. Measurements using Electrochemical Impedance Spectroscopy

Electrochemical impedance spectroscopy (EIS) is a method of investigation used in electrochemical systems. It is implemented usually in a potentiostat and assumes the superposition of a sinusoidal signal with small amplitude (5–10 mV) over a DC voltage and monitoring the magnitude and phase angle of the resulting ac current. The resulting impedance is usually represented as a complex quantity, as in (4):

$$Z(\omega) = Z'(\omega) + jZ''(\omega) \quad (4)$$

The EIS data can be represented in the complex plane as the so called Nyquist plots. The real part Z' and the imaginary part Z'' of the impedance are plotted in the complex plane, Z' being on the x-axis and Z'' on the y-axis, the resulting plot being a path (hodograph) having the frequency as parameter.

A typical Nyquist plot of a supercapacitor and of an ideal capacitor in series with a resistance is presented in Fig. 3.

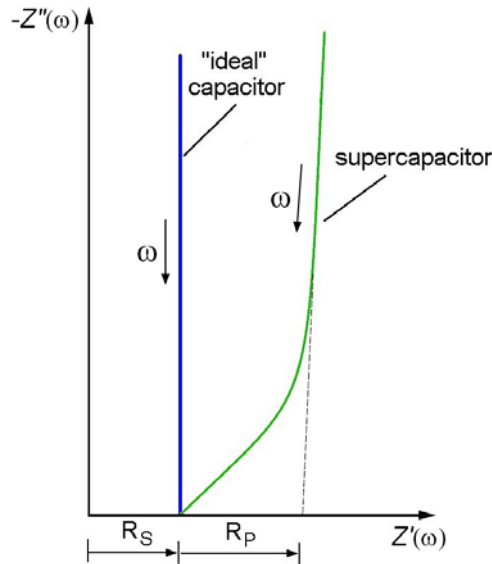


Fig. 3. Nyquist impedance plot of an ideal capacitor in series with a resistance R_s and a typical supercapacitor. The R_p value results from the restricted motion of ions

Another method to present the results is in form the impedance modulus and phase plotted versus frequency, the graphs being known as Bode plots.

It is usually to compare the EIS plots with known patterns of typical electric circuits or electrochemical components, or similar, to fit the data with the impedance of equivalent electronic circuits, the circuit elements having an equivalent to physical and chemical processes.

For instance, related to Fig. 3. for the ideal capacitor, the shift of the vertical line in the x axis direction identifies the equivalent series resistance (ESR) of the device under test and the vertical slope exhibits a capacitance that is invariant with frequency. In the same figure, the plot of a real supercapacitor shows two distinct regions: One is the region of the graph with a 45 degree slope, that region being encountered at higher frequencies. In electrochemical literature [4] the portion of the graph corresponds to diffusion process, related to the ability of ions to penetrate the pores, that is modeled by a distributed resistance R_p and a distributed capacitance.

In the lower frequency domain, the plot is an almost vertical line, showing the capacitive behavior of the component.

If the measurements are continued at higher frequencies, the imaginary part Z'' drops below the x -axis, showing an inductive character, modeled by a series inductance. For the presence of the inductance are responsible the wounded constructive structure of capacitor and the inductance of the test leads.

The capacitance of supercapacitor can be computed from the low frequency response, ie the Z'' part:

$$-Z'' = \frac{1}{\omega C} \quad (5)$$

Theoretical, a plot of $-Z''$ versus $1/\omega$ will be a straight line with slope $1/C$, this way the capacitance can be computed, as will be presented in Table 1.

In order to obtain reliable measured data, the applied ac signal must be small (few millivolts), so that the perturbation signal makes the system to remain in the linear domain. In this sense, the Kramers-Kronig (K-K) [5] relations are used to verify the conditions of linearity, causality, stability, and "finiteness" of impedance magnitude.

The Kramers-Kronig relations that are presented in equations (6) and (7), include two integral equations that govern the relationship between the real and imaginary parts of complex impedance for systems fulfilling the conditions mentioned above.

$$Z'(\omega) = Z'(\infty) + \frac{2}{\pi} \int_0^{\infty} \frac{xZ''(x) - \omega Z''(\omega)}{x^2 - \omega^2} dx \quad (6)$$

$$Z''(\omega) = -\frac{2\omega}{\pi} \int_0^{\infty} \frac{Z'(x) - Z'(\omega)}{x^2 - \omega^2} dx \quad (7)$$

with ω the angular frequency, x the integration variable.

The Kramers-Kronig equations can be used to validate the EIS measurements data and to reduce, if necessary, the frequency domain, eliminating the non-consistent data.

We have used this facility, because in our case, especially at higher frequencies the behavior of supercapacitors becomes inductive and we have to find the maximum frequency for which an equivalent RC circuit can be found. It is to mention that the impedance of circuits built with resistor, capacitances and inductances always satisfy the K-K relations.

The relations can be used, for instance to calculate one part of the impedance from the other part of the impedance that we suppose has been with higher accuracy experimentally measured.

For example, the imaginary part can be calculated from the experimentally measured real part of the impedance using Eq. (4). Then, we can compare the experimental data for Z'' with this calculated value. Differences between calculated and measured data will show that the measuring was altered either the system was outside linear domain or that were problems of causality or stability. There are, however difficulties in applying this method, because we need to integrate the known part of the impedance from zero to infinity, so the data set must be comprehensive and the function should be finite over the frequency range.

A method that does not require extrapolating data to extended frequency range, where measurement data could not been possible to obtain through experiments is to obtain the fit of the data with an equivalent RLC circuit.

The software implemented in the potentiostat used in our measurement can offer a measure of data confidence by computing a global error named "pseudo χ^2 ". In fact the K-K test consists in fitting the data with a special series of RC circuits (for impedance mode), that satisfies the K-K relations. The computed values of pseudo χ^2 are the sum of squares of individual residuals, see (8) and (9) for each data point.

$$\chi_{re}^2 = \sum_{i=1}^N \frac{[Z'_i - Z'(\omega_i)]^2}{|Z(\omega_i)|^2} \quad (8)$$

$$\chi_{im}^2 = \sum_{i=1}^N \frac{[Z''_i - Z''(\omega_i)]^2}{|Z(\omega_i)|^2} \quad (9)$$

$$\chi_{pseudo}^2 = \chi_{re}^2 + \chi_{im}^2 = \sum_{i=1}^N \frac{[Z'_i - Z'(\omega_i)]^2 + [Z''_i - Z''(\omega_i)]^2}{|Z(\omega_i)|^2} \quad (10)$$

In the formulae from above, Z'_i and Z''_i are experimental values and $Z'(\omega_i)$ and $Z''(\omega_i)$ are the fitted values.

From local experience, values of χ^2 below 10^{-3} shows a good fit and hence a good confidence factor. We have used this factor to check the proposed equivalent circuits of supercapacitors in Fig. 4.

III. Results

We have investigated 3 types of supercapacitors with different capacitance values: 5 F, 10 F and 22 F (see Fig. 5.) different temperature values: ambient temperature ($\sim 24^\circ\text{C}$), 80°C and 100°C . The aim of this monitoring was to see the behavior at different temperatures of these components. For this we held ten minutes at the maximum voltage (5.4 V, 2.5 V and 2.5 V) each component at each of the three temperatures for stabilization and for the correct creation of the double layer. After that, we have used a potentiostat to perform all the measurements. All data were monitored and tabulated by specialized software called Nova. The Nyquist plots for tested supercapacitors at $\sim 24^\circ\text{C}$ that we obtained with the Nova software is presented in the Fig. 5.

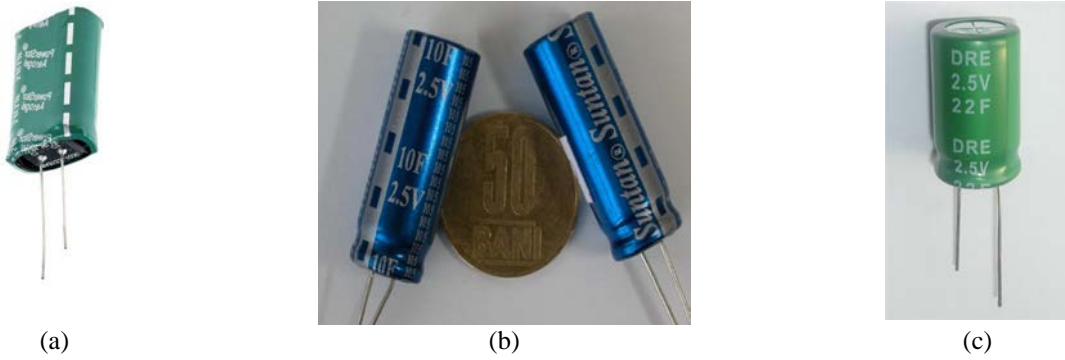


Fig. 6. The tested supercapacitors : (a) 5 F / 5.4 V, (b) 10 F / 2.5 V, (c) 22 F / 2.5 V

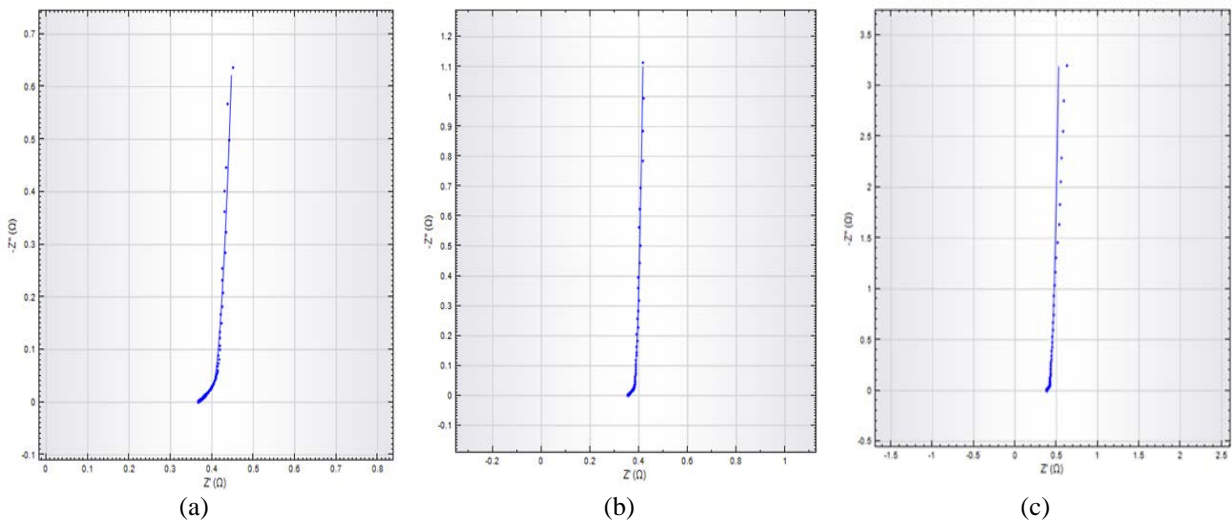


Fig. 5. Nyquist plots obtained with Nova software for supercapacitors at $\sim 24^\circ\text{C}$: (a) 5 F / 5.4 V, (b) 10 F / 2.5 V, (c) 22 F / 2.5 V

The variation of negative imaginary part of impedance function of time at different values of temperature ($\sim 24^\circ\text{C}$ - ambient temperature, 80°C and 100°C) for the tested supercapacitors is presented in the below figure. The temperature variation does not surprisingly affect the capacitance values for the three supercapacitors.

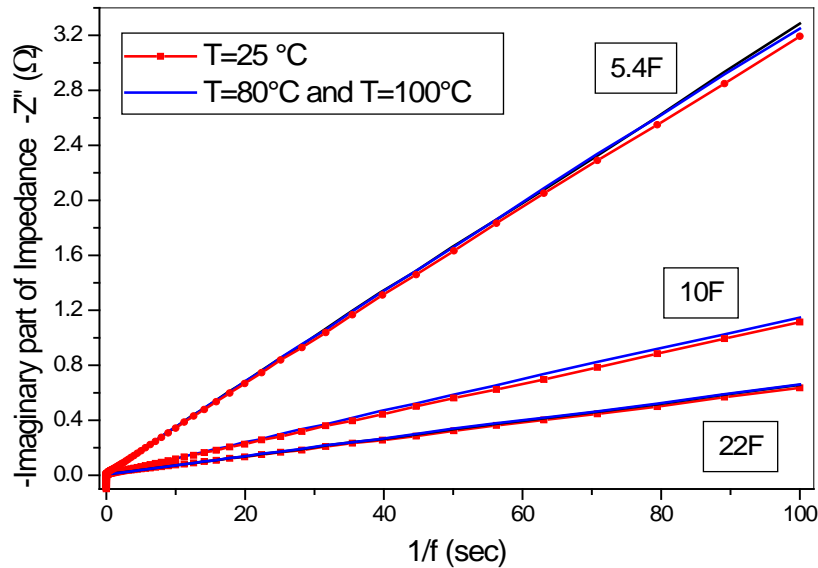


Fig. 7. The plot of the negative imaginary part of impedance function of time

For calculated the value of capacitance we used the equation (5) and we took into consideration the points in the plot that correspond to the time of 20 and 100 seconds and we calculated the slope of the straight line. The results are presented in Table 1.

Table 1. The calculated and fitted values of capacitance for tested supercapacitors

Temperature [°C]	Supercap-5F-5.4 V		Supercap-10F-2.5 V		Supercap-22F-2.5 V	
	$C_{calc.}[F]$	C_2 based on fitted measurements [F]	$C_{calc.}[F]$	C_2 based on fitted measurements [F]	$C_{calc.}[F]$	C_2 based on fitted measurements [F]
~ 24	5.04	5.1866	14.34	15.018	25.35	27.83
80	4.96	5.184	13.96	14.318	24.43	26.22
100	4.88	5.122	14.07	14.33	24.32	25.893
Temperature coefficient [ppm/°C]	-417		-247		-534	

The variation of real part of impedance with the different values of frequency for the supercapacitor 22F is presented in the Fig. 7. It can see that the values of real part of impedance are different at the three tested temperatures.

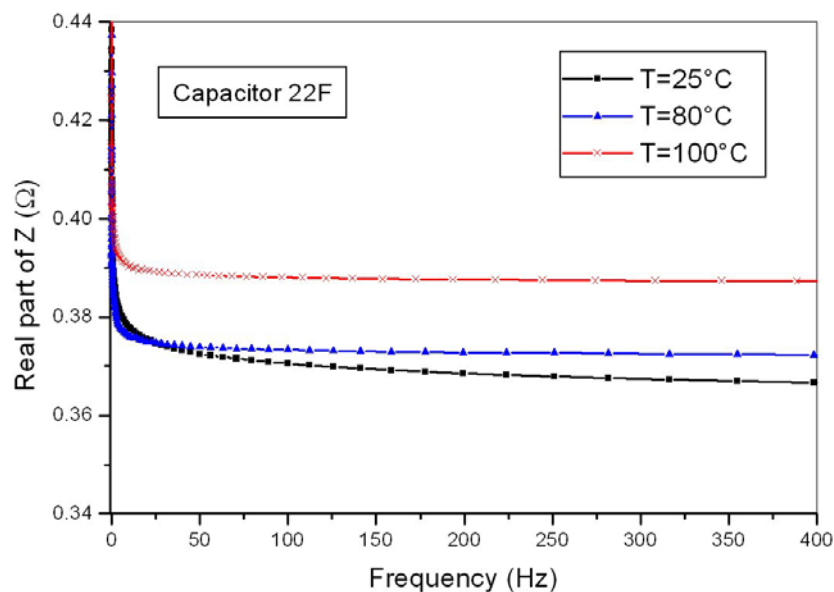


Fig. 7. The real part of impedance function of frequency

To identify the capacitance and the other parameters of superconductors, the values obtained by electrochemical impedance spectroscopy were made fitted using different equivalent circuits and choosing the most favorable variant in which for the pseudo χ^2 we obtained the lowest value (see Table 2). After many fitting attempts, the circuit for which the best fit was obtained is presented in Fig. 8.

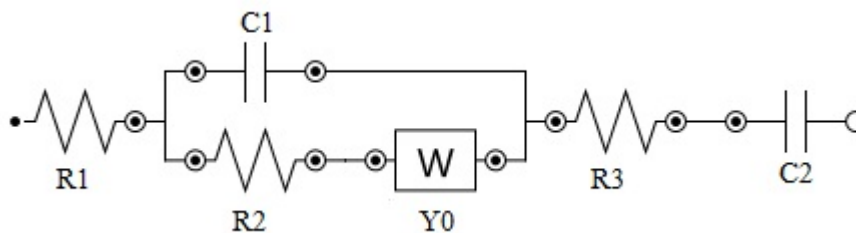


Fig. 8. The equivalent circuit used for fitting of EIS measurements

Table 2. The values of parameters obtained after the fitting for the tested supercapacitors

Parameters	Supercap-5F-5.4V			Supercap-10F-2.5V			Supercap-22F-2.5V		
	23.8°C	80°C	100°C	23.7°C	80°C	100°C	24.1°C	80°C	100°C
Temperature									
R_1 [Ω]	0.1907	0.39111	0.25	0.172	0.368	0.382	0.204	0.203	0.388
C_1 [F]	0.69101	0.61111	0.52235	2.134	1.969	1.823	2.706	3.652	3.656
R_2 [Ω]	0.0249	0.01366	0.01074	0.019	0.009	0.008	0.025	0.009	0.007
Y_0 [S]	23.273	23.973	20.43	72.02	80.67	72.61	56.843	72.367	73.691
R_3 [Ω]	0.19144	0	0	0.1865	0	0	0.1684	0.1708	0
C_2 [F]	5.1866	5.184	5.122	15.018	14.318	14.33	27.83	26.22	25.893
χ^2	0.00942	0.01264	0.02526	0.002623	0.002037	0.002527	0.00942	0.01264	0.02526

IV. Conclusions

We have investigated a series of supercapacitors using Electrochemical Impedance Spectroscopy method. As a novelty we have investigated the effect of temperature on supercapacitor parameters, especially the capacitance and equivalent series resistance (resistance of electrolyte solution).

The temperature does not have a significant influence on the capacity of the monitored superconductors. As the temperature increases, the capacity decreases, but not significantly. The temperature coefficient gives us the stabilization with the temperature for the tested supercapacitors.

It was observed an influence of temperature on series resistance of supercapacitors, the resistance increases at higher temperatures. Finding a suitable equivalent circuit has been found to be complicated since there is not sufficient reference in the literature on electrochemical impedance spectroscopy on supercapacitors, especially for high values of capacitances. For reasonable low measuring frequencies (10mHz), which corresponds to a period of 100s, the EIS measurements on supercapacitors with values in the range of 100F-600F were not possible, the data points showing random distribution, practically a measuring noise.

Acknowledgements

The authors would like to thank the professor Cristian PIRVU and the entire college of the Department of General Chemistry, Faculty of Applied Chemistry and Materials Science, Polithenica University of Bucharest to offer the required equipment for measurements.

References

- [1] Conway, B. E., "Electrochemical Supercapacitors: Scientific Fundamentals and Technological Applications".
- [2] Aiping Yu, Victor Chabot, and Jiujun Zhang, Electrochemical Supercapacitors for Energy Storage and Delivery Fundamentals and Applications, CRC Press, 2013.
- [3] Vadim F. Lvovich, Impedance Spectroscopy - Applications to Electrochemical and Dielectric Phenomena, Published by John Wiley & Sons, Inc., Hoboken, New Jersey,
- [4] C. Breitkopf, K. Swider-Lyons (Eds.), Springer Handbook of Electrochemical Energy, Springer-Verlag Berlin Heidelberg, 2017.
- [5] M. Orazem, B. Tribollet, Electrochemical Impedance Spectroscopy, Wiley, 2008. Chap. 22.
- [6] Gamry, Common Equivalent Circuit Models, part 3.